Colloid Polym Sci 275:661–671 (1997)

ORIGINAL CONTRIBUTION

H.J. Keh
J. Kuo

Effect of adsorbed polymers on the slow motion of an assemblage of spherical particles relative to a fluid

Received: 28 August 1996
Accepted: 23 January 1997

Prof. H.J. Keh (✉) · J. Kuo
Department of Chemical Engineering
National Taiwan University
Taipei 106-17 Taiwan, Republic of China

Abstract The effects of adsorbed polymers on the sedimentation of a homogeneous distribution of colloidal spheres and on the fluid flow through a bed of particles are investigated theoretically. The Reynolds number is assumed to be small, and the surface polymer layers are assumed to be thin with respect to the radius of particles and to the surface-to-surface spacing between neighboring particles. The effects of interaction of the individual particles are taken into explicit account by employing a fundamental cell-model representation which is known to provide good predictions for the motion of a swarm of spheres within a fluid in the absence of adsorbed polymers. To solve the Stokes flow equations within and outside the polymer layer a method of matched asymptotic expansions in a small parameter λ is used, where λ is the ratio of the length scale of the polymer layer to the particle radius. The results for the sedimentation rate and the pressure drop are expressed in terms of an effective hydrodynamic thickness (L) of the polymer layer, which are accurate to $O(\lambda^2)$. When the concentration of particles in a suspension or a bed is increased, L becomes larger, meaning the settling velocity decreases or the pressure drop increases. The $O(\lambda)$ term for L normalized by its value in the limit $\lambda \to 0$ is found to be independent of the polymer segment distribution, the hydrodynamic interactions among the segments, and the volume fraction of the segments. The $O(\lambda^2)$ term for L, however, is a sensitive function of the polymer segment distribution and the volume fraction of the segments. In general, the particle-interaction effects on the motion of polymer-coated particles relative to a fluid can be quite significant.

Key words Suspension of colloidal spheres – adsorbed polymers – sedimentation velocity – particle interactions – cell model

Introduction

Adsorption of macromolecules from solution onto solid interfaces has long been a subject of both theoretical [1–6] and experimental [7–12] interest. Coating of colloidal particles with polymers plays an important role in the control of the stability/flocculation behavior of colloidal suspensions [13]. The interactions between polymer and particle generate nonuniform distributions of polymer throughout the solution and influence the energy between particles. Another spectacular effect of such adsorption is the restriction of flow in capillary pores due to the effective decrease in size [14]. This effect is strongly connected with

Colloid & Polymer Science, Vol. 275, No. 7 (1997)

many technologically important processes such as ultrafiltration, gel permeation chromatography, and tertiary oil recovery.

The structure of an adsorbed polymer layer depends on the nature of the polymer, the solvent, and the interface. In general, adsorbed polymer molecules have only part of their segments on the interface while a substantial fraction of the segments are protruding into the solution. Some segments on the interface are present in "trains" of variable length, the others are in "loops" (with both ends in contact with the interface), and in one or two "tails" at the end of the adsorbed molecule [15]. Since the adsorbed polymer layer is diffuse, there is no unique measure of its thickness. One convenient definition, applicable to both colloidal particles and micropores, is the hydrodynamic thickness which is the distance the "no-slip" boundary condition on the fluid velocity must be moved into the fluid phase to produce the same hydrodynamic effect as the polymer layer. For the case of a polymer layer that is thin relative to the radii of curvature of the solid surface, previous theoretical analyses [16, 17] predict the same value of the hydrodynamic thickness for different external flows and geometries, given the same local rheological model for flow within the surface layer.

The effects of adsorbed polymers on the steady translation of a single spherical particle were determined by Anderson and Kim [17] using a method of matched asymptotic expansions to solve the Stokes flow equations within and outside the polymer layer. The result for the drag force produced by the fluid on the particle, expressed as the hydrodynamic thickness of the adsorbed polymer layer, is accurate to $O(\lambda^2)$ where λ is the ratio of the polymer-layer length scale to the particle radius. Their calculations indicated that (i) the $O(\lambda^2)$ term is negative, meaning the hydrodynamic thickness decreases as the particle radius decreases assuming all other conditions are constant, (ii) the free-draining assumption for flow through the polymer chains applies accurately for calculating the hydrodynamic thickness if the Stokes radius of the polymer segments is much smaller than the length scale of the polymer layer, and (iii) the presence of only a small amount of adsorbed polymer tails can make a significant contribution to the hydrodynamic thickness if the length scale of the tails exceeds the length scale of the loops by a factor of two or more.

In most practical applications of particle motion relative to a fluid, collections of particles are encountered. Thus, it is important to determine if the presence of neighboring particles significantly affects the movement of particles. Using a far-field approximate technique, Anderson and Solomentsev [18] analytically solved the mobility problem of two arbitrarily oriented, identical spheres accounting for the presence of the surface layers on the particles. The mobility coefficients accurate to $O(\lambda^2)$ were determined in a power series of h^{-1} up to $O(h^{-5})$, where h is the center-to-center distance between the particles divided by their radius. Based on a microscopic model of particle interactions in a dilute dispersion which involves the statistical concept [19, 20], these mobility coefficients can be used to evaluate approximately the mean settling velocity in a dilute suspension of identical polymer-coated spheres as a function of the particle concentration, as is shown in the Appendix.

Another technique which has been employed successfully to predict the effect of particle concentration on sedimentation rate is the cell model [21–23]. The model involves the concept that an assemblage can be divided into a number of identical cells, one sphere occupying each cell. The boundary-value problem for multiple spheres is thus reduced to the consideration of the behavior of a single sphere and its bounding envelope. Although different shapes of cells can be employed, the assumption of a spherical shape for the fictitious envelope of fluid surrounding each spherical particle is of great convenience. The cell model is of great applicability in concentrated assemblages, where the effect of container walls will not be important. In this work, the cell model is used to describe the hydrodynamic interactions among spherical particles coated with polymer layers moving relative to a fluid. The solution obtained with this model enables the sedimentation rate in a concentrated suspension of identical particles or alternatively the pressure drop for fluid flow through a bed of particles to be predicted as a function of fractional void volume.

Analysis

We consider the sedimentation of a homogeneous distribution of identical spherical particles of radius R_1 in an incompressible Newtonian fluid. The surface of each particle is covered by a layer of adsorbed polymers. The thickness of the polymer layer is characterized by a length scale δ (based on loops if both loops and tails are present), which is assumed to be small in comparison with R_1 and with the surface-to-surface distance between two neighboring particles. So, any two thin polymer layers will not overlap with each other. In general, the length scale of a surface polymer layer depends on the molecular weight of the polymer, the amount of the polymer adsorbed, and the relative interactions among the polymer, interface, and fluid. The settling velocity of the particles equals $U\mathbf{e}_z$, where $\mathbf{e}_z$ is the unit vector in the positive z (gravitational) direction. The Reynolds number is assumed to be small.

The flow field in the fluid phase surrounding the particles is governed by the modified Stokes equations [17]:

$$\nabla \cdot \{\mu[\nabla \mathbf{v} + (\nabla \mathbf{v})^{\mathrm{T}}]\} - \nabla p - \zeta \rho f[\mathbf{v} - \mathbf{v}^{(p)}] = \mathbf{0},$$

$$\nabla \cdot \mathbf{v} = 0. \tag{1a,b}$$

Here, $\mathbf{v}$ is the fluid velocity, p is the hydrodynamic pressure, ζ is the friction coefficient of an isolated polymer segment, ρ is the density of polymer segments at the position in question, $\mathbf{v}^{(p)}$ is the velocity of the segments, f is a function of ρ accounting for the hydrodynamic interactions among the segments, and μ is the local fluid viscosity which also varies with ρ. The density distribution of the segments in the loops and tails cannot yet be determined experimentally. Previous theoretical studies [2,4] established that the density of polymer segments in the loops decays exponentially with the distance from the solid surface and the segment density in the tails can exceed the value in the bulk solution much farther from the surface. For a free-draining model for flow through the segments $f = 1$, while segment–segment interactions cause f to increase with ρ. It is understood that $\mathbf{v}^{(p)} = U\mathbf{e}_z$ in the surface layer surrounding each settling particle.

Following Happel [21] and Kuwabara [22] we take a cell model in which each particle is envisaged to be surrounded by a concentric spherical shell of fluid having an outer radius R_2 such that the cell contains the same volumetric proportion of solid to fluid as exists in the entire suspension (i.e., the volume fraction of the particles $\varphi = R_1^3/R_2^3$). Each particle is surrounded by a layer of adsorbed polymers, contained within the cell. On the outer boundary of the imaginary spherical shell, the Happel model assumes that the radial velocity and the shear stress are zero, while the Kuwabara model assumes that the radial velocity and the vorticity are zero. Both models give essentially the same velocity fields and approximately equal drag forces for the motion of a "bare" particle. However, the Happel model has a significant advantage in that it does not require an exchange of mechanical energy between the cell and the environment [23].

Since the flow field in a cell is axially symmetric, it is convenient to introduce the Stokes stream function Ψ which satisfies Eq. (1b) and is related to the velocity components in the spherical coordinate system (r, θ, ϕ), with its origin at the particle center, by

$$v_r = -\frac{1}{r^2 \sin\theta}\frac{\partial \Psi}{\partial \theta}, \qquad v_\theta = \frac{1}{r \sin\theta}\frac{\partial \Psi}{\partial r}. \tag{2a,b}$$

Taking the curl of Eq. (1a) and applying Eqs. (1b) and (2) gives a fourth-order linear partial differential equation for Ψ:

$$\mu E^4 \Psi + 2\frac{\mathrm{d}\mu}{\mathrm{d}r}\frac{\partial}{\partial r}(E^2\Psi) + 2\left(r\frac{\mathrm{d}^2\mu}{\mathrm{d}r^2} - \frac{\mathrm{d}\mu}{\mathrm{d}r}\right)\frac{\partial}{\partial r}\left(\frac{1}{r}\frac{\partial \Psi}{\partial r}\right) - \frac{\mathrm{d}^2\mu}{\mathrm{d}r^2}E^2\Psi - \lambda^{-2}\left(\beta E^2\Psi + \frac{\mathrm{d}\beta}{\mathrm{d}r}\frac{\partial \Psi}{\partial r}\right) = 0, \tag{3}$$

where the dimensionless parameters β and λ are defined as

$$\beta = \frac{\delta^2 \zeta \rho f}{\mu_s}, \qquad \lambda = \frac{\delta}{R_1}, \tag{4a,b}$$

and the axisymmetric Stokesian operator E^2 is given by

$$E^2 = \frac{\partial^2}{\partial r^2} + \frac{\sin\theta}{r^2}\frac{\partial}{\partial \theta}\left(\frac{1}{\sin\theta}\frac{\partial}{\partial \theta}\right). \tag{5}$$

In Eq. (3), dimensionless variables are used, with r normalized by the radius R_1, μ by the solvent viscosity μ_s, and Ψ by UR_1^2. The parameter β denotes the ratio of the frictional force exerted by the polymer segments on the fluid to the viscous force of the bulk fluid, and is O(1) with respect to λ which has been assumed to be small. Equation (3) must be solved subject to the following boundary conditions:

$$r = R_1: \quad \mathbf{v} = U\mathbf{e}_z, \tag{6a}$$

$$r = R_2: \quad v_r = 0, \tag{6b}$$

$$r = R_2: \quad \tau_{r\theta} = \mu r \frac{\partial}{\partial r}\left(\frac{v_\theta}{r} + \frac{1}{r}\frac{\partial v_r}{\partial \theta}\right) = 0. \tag{6c}$$

Here, the Happel model for the boundary conditions on the outer envelope of the cell is employed.

The drag force (in the z direction) acting on the particle surface $r = R_1$ is [23]

$$F_d = \pi \mu_s \int_0^\pi r^3 \sin^3\theta \frac{\partial}{\partial r}\left(\frac{E^2\Psi}{r^2 \sin^2\theta}\right) r\,\mathrm{d}\theta. \tag{7}$$

In terms of the equivalent hydrodynamic thickness L of the adsorbed polymer layer surrounding the particle, the drag force is given by the Stokes law with an envelope-boundary correction,

$$F_d = -6\pi\mu_s(R_1 + L)UK. \tag{8}$$

For the system specified by Eq. (6), the envelope-boundary correction factor $K = -4D_0/3R_1$ where D_0 is defined by Eq. (12b). The hydrodynamic thickness of the polymer layer can be expressed as

$$L = AR_1\lambda(1 + B\lambda) + \mathrm{O}(\lambda^3). \tag{9}$$

By combining Eqs. (7)–(9) after solving Eqs. (3) and (6) for Ψ, one can obtain dimensionless parameters A and B. Note that $K \geq 1$, A is positive, and B represents the correction for the particle curvature.

Equation (3) poses a singular perturbation problem when $\lambda \ll 1$. In the "outer region", where $r - R_1 \gg R_1\lambda$, one has $\mu = \mu_s$ and $\beta = 0$ and the solution can be written as

$$\Psi^{(O)} = (Cr^{-1} + Dr + Er^2 + Fr^4)U \sin^2\theta \,, \tag{10}$$

$$C = C_0 + \lambda C_1 + \lambda^2 C_2 + \cdots \,, \tag{11a}$$

$$D = D_0 + \lambda D_1 + \lambda^2 D_2 + \cdots \,, \tag{11b}$$

$$E = E_0 + \lambda E_1 + \lambda^2 E_2 + \cdots \,, \tag{11c}$$

$$F = F_0 + \lambda F_1 + \lambda^2 F_2 + \cdots \,. \tag{11d}$$

The constants C_0, D_0, E_0, and F_0 can be obtained by solving for the corresponding motion of a "bare" spherical particle in a spherical envelope, with the result

$$C_0 = \tfrac{1}{4}R_1^3\varpi, \qquad D_0 = -\tfrac{1}{4}R_1(3 + 2l^5)\varpi \,, \tag{12a,b}$$

$$E_0 = \tfrac{1}{4}(3l + 2l^6)\varpi, \qquad F_0 = -\tfrac{1}{4}R_1^{-2}l^3\varpi \,, \tag{12c,d}$$

where

$$l = \frac{R_1}{R_2} = \varphi^{1/3}, \qquad \varpi = (1 - \tfrac{3}{2}l + \tfrac{3}{2}l^5 - l^6)^{-1}. \tag{13a,b}$$

The unknown constants C_n, D_n, E_n, and F_n for $n \geq 1$ are to be determined by matching $\Psi^{(O)}$ with the solution to Eq. (3) in the "inner region". Combination of Eqs. (7)–(11) results in

$$A = \frac{D_1}{D_0}, \qquad B = \frac{D_2}{D_1} \,. \tag{14a,b}$$

Within the "inner region" adjacent to the particle, where $r - R_1 \sim O(R_1\lambda)$, a solution to Eq. (3) with the reference frame moving with the particle is sought in the form

$$\Psi^{(I)} = [\lambda^2 F_2(y) + \lambda^3 F_3(y) + \cdots]U \sin^2\theta \,, \tag{15}$$

where the variable $y = \lambda^{-1}(r - R_1)$. Substituting Eq. (15) into Eqs. (3) and (6a) and collecting terms of equal orders in λ generates the following equations for $F_n(y)$ up to $n = 3$:

$$\frac{R_1}{\mu_s}\frac{d}{dy}\left(\mu\frac{d^2F_2}{dy^2}\right) - \frac{\beta}{R_1}\frac{dF_2}{dy} = 0 \,, \tag{16a}$$

$$y = 0: \quad F_2 = \frac{dF_2}{dy} = 0 \,; \tag{16b}$$

$$\frac{R_1}{\mu_s}\frac{d}{dy}\left(\mu\frac{d^2F_3}{dy^2}\right) - \frac{\beta}{R_1}\frac{dF_3}{dy} = \frac{2}{\mu_s}\frac{d\mu}{dy}\frac{dF_2}{dy} - c \,, \tag{17a}$$

$$y = 0: \quad F_3 = \frac{dF_3}{dy} = 0 \,, \tag{17b}$$

where c is an integration constant to be determined by matching the inner and outer solutions.

The unknown boundary conditions on F_n at $y \to \infty$ and the unknown constants C_n, D_n, E_n, and F_n can be obtained by matching Eqs. (10) and (15) at equivalent orders in λ:

$$\lim_{y\to\infty} \Psi^{(I)} = \lim_{y\to\infty} [\Psi^{(O)} + \tfrac{1}{2}Ur^2 \sin^2\theta]_{r = R_1 + \lambda y} \,. \tag{18}$$

In Eq. (18), the second term in brackets accounts for the difference in the reference frames used for $\Psi^{(I)}$ and $\Psi^{(O)}$. After completing this matching we obtain the following equations:

$$0 = W_0 + \tfrac{1}{2}R_1^2, \quad 0 = W_1 + yX_0 + R_1 y \,, \tag{19a,b}$$

$$\lim_{y\to\infty} F_2 = W_2 + yX_1 + y^2Y_0 + \tfrac{1}{2}y^2 \,, \tag{19c}$$

$$\lim_{y\to\infty} F_3 = W_3 + yX_2 + y^2Y_1 + y^3Z_0 \,, \tag{19d}$$

where

$$W_k = R_1^{-1}C_k + R_1D_k + R_1^2E_k + R_1^4F_k \,, \tag{20a}$$

$$X_k = -R_1^{-2}C_k + D_k + 2R_1E_k + 4R_1^3F_k \,, \tag{20b}$$

$$Y_k = R_1^{-3}C_k + E_k + 6R_1^2F_k \,,$$

$$Z_k = -R_1^{-4}C_k + 4R_1F_k \,, \tag{20c,d}$$

for $k = 0$, 1, 2, or 3.

Equation (19a) and the derivative of Eq. (19b) with respect to y are immediately satisfied with the solution of C_0, D_0, E_0, and F_0 given by Eq. (12). The constants C_1, D_1, E_1, and F_1 can be determined by solving Eq. (19b) and the derivative of Eq. (19c) with the knowledge of C_0, D_0, E_0, and F_0, and then the constants C_2, D_2, E_2, and F_2 are to be determined by solving Eq. (19c) and the derivative of Eq. (19d). The useful results are

$$D_1 = -\tfrac{1}{3}R_1b^2\gamma \,, \tag{21a}$$

$$D_2 = \tfrac{1}{3}\lim_{y\to\infty}\left[b\left(\frac{dF_3}{dy} + c\frac{y^2}{2R_1} - dy\right) + c\left(\frac{F_2}{R_1} - b\frac{y^2}{2R_1} + b\gamma y\right)\right], \tag{21b}$$

where

$$\gamma = \frac{1}{R_1}\lim_{y\to\infty}\left(-\frac{1}{b}\frac{dF_2}{dy} + y\right) \tag{22}$$

and

$$b = \tfrac{3}{2}(1 - l^5)\varpi\,, \quad c = \tfrac{3}{2}(1 + 4l^5)\varpi\,,$$

$$d = (1 - 6l^5 + 5l^6)b\gamma\varpi\,. \tag{23a,b,c}$$

Taking the differentiation of Eqs. (19c) and (19d) with respect to y twice, we obtain

$$\lim_{y\to\infty}\frac{d^2F_2}{dy^2} = b\,, \qquad \lim_{y\to\infty}\frac{d^2F_3}{dy^2} = -c\frac{y}{R_1} + d\,. \tag{24a,b}$$

Knowing that $\mu = \mu_s$ and $\beta = 0$ as $y \to \infty$, one can find that Eqs. (16a) and (17a) are consistent with Eq. (24).

If we define new variables

$$G = -\frac{1}{b}\frac{dF_2}{dy}, \qquad H = -\frac{1}{c}\frac{dF_3}{dy}\,, \tag{25a,b}$$

then Eqs. (16), (17), and (24) give

$$\frac{R_1}{\mu_s}\frac{d}{dy}\left(\mu\frac{dG}{dy}\right) - \frac{\beta}{R_1}G = 0\,, \tag{26a}$$

$$y = 0: \quad G = 0\,, \tag{26b}$$

$$y \to \infty: \quad \frac{dG}{dy} \to -1\,; \tag{26c}$$

$$\frac{R_1}{\mu_s}\frac{d}{dy}\left(\mu\frac{dH}{dy}\right) - \frac{\beta}{\mu}H = 1 + 2\frac{b}{c}\frac{G}{\mu_s}\frac{d\mu}{dy}\,, \tag{27a}$$

$$y = 0: \quad H = 0\,, \tag{27b}$$

$$y \to \infty: \quad \frac{dH}{dy} \to \frac{y}{R_1} - \frac{d}{c}\,. \tag{27c}$$

The two parameters of Eq. (9) are obtained from Eqs. (14) and (21):

$$A = -\frac{b^2}{3D_0}\lim_{y\to\infty}(G + y)\,, \tag{28a}$$

$$B = -\frac{bc}{3D_0A}\left[\lim_{y\to\infty}\left(H - \frac{y^2}{2R_1} + \frac{d}{c}y\right) + \frac{1}{R_1}\int_0^\infty (G + y - R_1\gamma)\,dy\right]. \tag{28b}$$

After obtaining the solutions of Eqs. (26) and (27) for given polymer segment density distributions $\rho(y)$ and the dependence of μ and β on ρ, parameters A and B can be evaluated from Eq. (28).

In the limit of $R_2/R_1 \to \infty$ (an infinitely dilute suspension), the boundary effect of the envelope on the motion of the particle disappears. For this case, Eq. (23) gives $b = c = 3/2$ and $d = (3/2)\gamma_\infty$, and Eq. (28) reduces to

$$A_\infty = \gamma_\infty = \frac{1}{R_1}\lim_{y\to\infty}(G_\infty + y)\,, \tag{29a}$$

$$B_\infty = \frac{1}{R_1\gamma_\infty}\lim_{y\to\infty}\left(H_\infty - \frac{y^2}{2R_1} + \gamma_\infty y\right) + \frac{1}{R_1^2\gamma_\infty}\int_0^\infty (G_\infty + y - R_1\gamma_\infty)\,dy\,. \tag{29b}$$

Here, we use the subscript "∞" to denote the limiting case of $R_2/R_1 \to \infty$. Both theoretical calculations [17] and experimental data [9–11] showed that the value of B_∞ would be negative, meaning the hydrodynamic thickness of the adsorbed polymer layer increases with particle radius assuming all other conditions are constant.

The drag force exerted on the particle written by Eq. (8) can also be expressed as

$$F_d = -6\pi\mu_s(R_1 + L_\infty)UK[1 + g\lambda + h\lambda^2 + O(\lambda^3)]\,, \tag{30}$$

where

$$L_\infty = A_\infty R_1\lambda(1 + B_\infty\lambda) + O(\lambda^3)\,. \tag{31}$$

Here, the hydrodynamic thickness of the polymer layer surrounding the particle is taken to be a constant equal to the value when the envelope boundary is not present (L_∞), and the envelope-boundary correction is given by an expansion in λ. A comparison between Eqs. (8) and (30) yields

$$g = A - A_\infty, \quad h = AB - A_\infty B_\infty - A_\infty(A - A_\infty)\,. \tag{32a,b}$$

If we use U_∞ to denote the settling velocity of the particle in the limit of $R_2/R_1 \to \infty$, then the relation between U and U_∞ can be written as

$$\frac{U}{U_\infty} = \frac{1 + A_\infty\lambda + A_\infty B_\infty\lambda^2 + O(\lambda^3)}{K[1 + A\lambda + AB\lambda^2 + O(\lambda^3)]} = K^{-1}[1 + g\lambda + h\lambda^2 + O(\lambda^3)]^{-1}\,. \tag{33}$$

In the following section, numerical calculations show that $A > A_\infty$ (or $g > 0$), and then $U/U_\infty < 1$, for all cases with a finite value of R_2/R_1.

The cell model can also be applied to the case of fluid flow through a bed of particles (or a porous medium) in the presence of adsorbed polymer layers. For the model under consideration, the drag force F_d divided by the cell volume $(4/3)\pi R_2^3$ will equal $-\Delta p/L_b$, the pressure drop per unit

length of bed due to passage of fluid through it. Use of this relationship and Eqs. (8) and (9) gives

$$U = \left\{K^{-1}[1 + A\lambda + AB\lambda^2 + O(\lambda^3)]^{-1}\frac{2R_1^2}{9l^3}\right\}\frac{\Delta P}{\mu_s L_b}, \quad (34)$$

where U is the superficial fluid velocity through the bed. The expansion in braces is the permeability coefficient in the well-known Darcy law. If we use U_∞ and ΔP_∞ to represent U and ΔP, respectively, in the limit of $R_2/R_1 \to \infty$ (a dilute medium), the ratio U/U_∞ with $\Delta P = \Delta P_\infty$ (equals the ratio $\Delta P_\infty/\Delta P$ with $U = U_\infty$) can also be expressed by Eq. (33).

When the Kuwabara model for the boundary conditions on the outer envelope of the cell is used, Eq. (6c) becomes

$$r = R_2: \quad (\nabla \times \mathbf{v})_\phi = \frac{\partial v_\theta}{\partial r} + \frac{v_\theta}{r} - \frac{1}{r}\frac{\partial v_r}{\partial \theta} = 0 . \quad (35)$$

With this change, the above analysis is still valid except that Eq. (12) is replaced by [22, 24]

$$C_0 = \tfrac{1}{20}R_1^3(5 - 2l^3)\varpi', \qquad D_0 = -\tfrac{3}{4}R_1\varpi' , \quad (36a,b)$$

$$E_0 = \tfrac{1}{20}(18l - 5l^3 + 2l^6)\varpi', \quad F_0 = -\tfrac{3}{20}R_1^{-2}l^3\varpi' , \quad (36c,d)$$

and Eq. (23) is replaced by

$$b = \tfrac{3}{2}(1 - l^3)\varpi', \quad c = \tfrac{3}{2}(1 - 2l^3)\varpi', \quad d = (1 - l^3)^2 b\gamma\varpi'. \quad (37a,b,c)$$

Here,

$$\varpi' = (1 - \tfrac{9}{5}l + l^3 - \tfrac{1}{5}l^6)^{-1} . \quad (38)$$

Note that, for the Happel model,

$$K^{-1} = 1 - \tfrac{3}{2}\varphi^{1/3} + O(\varphi^{5/3}) ; \quad (39a)$$

for the Kuwabara model,

$$K^{-1} = 1 - \tfrac{9}{5}\varphi^{1/3} + O(\varphi) . \quad (39b)$$

Results and discussion

The results for the sedimentation of a homogeneous distribution of colloidal spheres and for the fluid through a bed of particles in the presence of adsorbed polymer layers are presented in this section. The two hydrodynamic parameters A and B required by Eq. (33) are calculated from Eq. (28) in which the variables G and H can be obtained by numerically solving Eqs. (26) and (27) in sequence. The only polymer-layer properties that are required are μ and β, which should be related to the segment density $\rho(y)$ by an appropriate hydrodynamic model. Previous calculations for an isolated sphere [17] have shown that the effects of $\mu > \mu_s$ are negligible compared to the effects of β. Therefore, we assume $\mu = \mu_s$ throughout the polymer layers in this and the following sections.

Following Anderson and Kim [17], we assume that the segment density has a form of two exponentially decaying distributions,

$$\rho(y) = \rho_0(e^{-y/\delta} + \eta e^{-\alpha y/\delta}) , \quad (40)$$

where the primary distribution ($\rho_0 e^{-y/\delta}$) represents segments in the loops and the secondary distribution denotes the tails. α is the ratio of loop-to-tail length scales for the polymer layer and is smaller than unity. It can be found from Eq. (40) that the fraction of segments contained in the tails is $\eta/(\eta + \alpha)$. Theories based on lattice statistics [2–4, 25] have shown that the segment density in tails increases with the distance from the interface, then passes through a maximum, followed by an exponential decrease with a decay length which is about twice (or more in some cases) that of the segment density in loops. At very small distances from the interface the loops prevail over the tails, while the outer part of the adsorbed layer is completely dominated by the tails. The function form expressed by Eq. (40) is a simple and reasonable approximation for the segment density distribution as long as η and α are small (say, $\eta/(\eta + \alpha) \leq 0.3$ and $\alpha \leq 0.5$).

Substituting Eq. (40) into Eq. (4a) yields

$$\beta(y) = \beta_0(e^{-y/\delta} + \eta e^{-\alpha y/\delta})f , \quad (41)$$

where

$$\beta_0 = \frac{\delta^2\zeta\rho_0}{\mu_s} = \frac{9}{2}\left(\frac{\delta}{a}\right)^2\phi_0 , \quad (42)$$

a ($=\zeta/6\pi\mu_s$) is the Stokes radius of each segment, and ϕ_0 ($=4\pi a^3\rho_0/3$) represents the volume fraction of segments based on the segment density at the surface of a particle. For reasonable adsorption energies (i.e. not very close to the adsorption/desorption transition), ϕ_0 is of order (but obviously below) unity. With the assumption that $\delta/a \gg 1$, the typical values of β_0 are expected to be in the range $10 \sim 1000$.

The hydrodynamic parameters A and B for a polymer-coated particle normalized by their values in the absence of others (A_∞ and B_∞) can be evaluated for a given distribution of β as expressed by Eq. (41). In our calculations, the Runge–Kutta–Fehlbery method [26] was employed to obtain the numerical solutions of the variables G and H. Also, only the results obtained by using the Happel model for the boundary conditions on the outer envelope of the

Table 1 Numerical results of A/A_∞ and B/B_∞ for the motion of a swarm of polymer-coated spheres relative to a fluid with various values of parameters φ and β_0 for systems with no polymer tails in the free-draining limit

$\varphi^{1/3}$	φ	A/A_∞	$-B/B_\infty$			K
			$\beta_0 = 10$	$\beta_0 = 100$	$\beta_0 = 1000$	
0	0	1	−1	−1	−1	1
0.1	0.001	1.176	−0.359	0.778	2.484	1.176
0.2	0.008	1.426	0.539	3.272	7.372	1.428
0.3	0.027	1.797	1.811	6.819	14.33	1.812
0.4	0.064	2.366	3.602	11.86	24.24	2.448
0.5	0.125	3.269	6.129	19.06	38.46	3.630
0.6	0.216	4.757	9.808	29.73	59.61	6.188
0.7	0.343	7.369	15.64	46.95	93.92	13.17
0.8	0.512	12.63	26.72	80.21	160.5	41.48
0.9	0.729	28.02	58.69	177.3	355.3	324.6
0.95	0.857	58.26	121.7	369.6	741.6	2616
0.99	0.970	298.5	623.6	1903	3824	3.3E5

$B_0 = 10$: $A_\infty = 3.4570$, $B_\infty = -0.9509$.
$B_0 = 100$: $A_\infty = 5.7596$, $B_\infty = -0.5712$.
$B_0 = 1000$: $A_\infty = 8.0622$, $B_\infty = -0.4081$.

cell will be presented. In general cases, the predictions of Happel's model and Kuwabara's model are in numerical agreement to within 15% and result in the same behavior qualitatively.

Results of A/A_∞ and B/B_∞ for various values of the volume fraction of particles are given in Table 1 for systems with no tails ($\eta = 0$) in the free-draining limit ($f = 1$). Three constant values 10, 100, and 1000 are chosen for the parameter β_0 and the values of A_∞ and B_∞ for each case are also listed in this table. Note that, although A_∞ is a function of β_0, the ratio A/A_∞ (or g/A_∞) is independent of this parameter. As expected, the particle interactions increase the value of A and the ratio A/A_∞ (or g/A_∞) increases monotonically and rapidly with the increase of the volume fraction of particles. In the limit $\varphi \to 0$, there is no particle interaction effect and $A = A_\infty$. On the other hand, the ratio B/B_∞ decreases monotonically from unity and soon becomes negative (or the value of B increases monotonically from B_∞, which is negative, and soon becomes positive) when φ increases from zero. Namely, the hydrodynamic thickness of the adsorbed polymer layer (or the surface-layer-enhanced frictional drag on a particle) increases as the particle radius decreases assuming that the volume fraction of particles and all other conditions are constant. Although the magnitude of B_∞ decreases with the increase of β_0, the magnitude of B or B/B_∞ increases with the increase of β_0 for the general case. In agreement with the above theoretical predictions, experimental results for titanium dioxide particles covered by adsorbed polymers showed that the hydrodynamic thickness of the surface layer increases with the increase of the volume fraction of particles [8].

For convenience in using Eqs. (8), (30), (33), and (34) to evaluate the drag force or settling velocity of a particle and the superficial fluid velocity or pressure drop through a bed of particles, we also list the values of K as a function of φ in Table 1. It can be seen from Eq. (33) and Table 1 that the ratio U/U_∞ decreases monotonically from unity with the increase of φ from zero. In the Appendix, an analytical expression relating U/U_∞ to φ is obtained (given by Eqs. (A1) and (A6)) by an alternative method using the far-field approximate solution for the mobility problem of two polymer-coated spheres [18]. This expression also shows that U/U_∞ is a monotonic decreasing function of φ. Note that the particle interaction effect on the settling velocity or the pressure drop illustrated in Table 1 is very significant when φ approaches unity.

We next consider the effect of tails in the adsorbed polymer layer surrounding a particle. Equations (26) and (27) are solved for G and H in the free-draining limit over a range of η and α. The results of parameters B and h as a function of the ratio $\varphi^{1/3}$ are plotted in Fig. 1 for typical cases of the fraction of polymer segments contained in the tails, $\eta/(\eta + \alpha)$. The curve of parameter A (or g) is not drawn since the ratio A/A_∞ is not a function of $\eta/(\eta + \alpha)$ or α and its results were presented in Table 1. It is clear that the increase of the segment fraction in the tails or the increase of the relative length of the tails (with a decrease in α) will increase the particle interaction effect on B and h when all the other conditions are unchanged. This influence can be quite significant when the value of α is less than 0.5.

We have also numerically solved for G and H for the system with no tails in the adsorbed polymer layers considering the hydrodynamic interactions among the polymer segments. In the calculations, we follow Anderson and

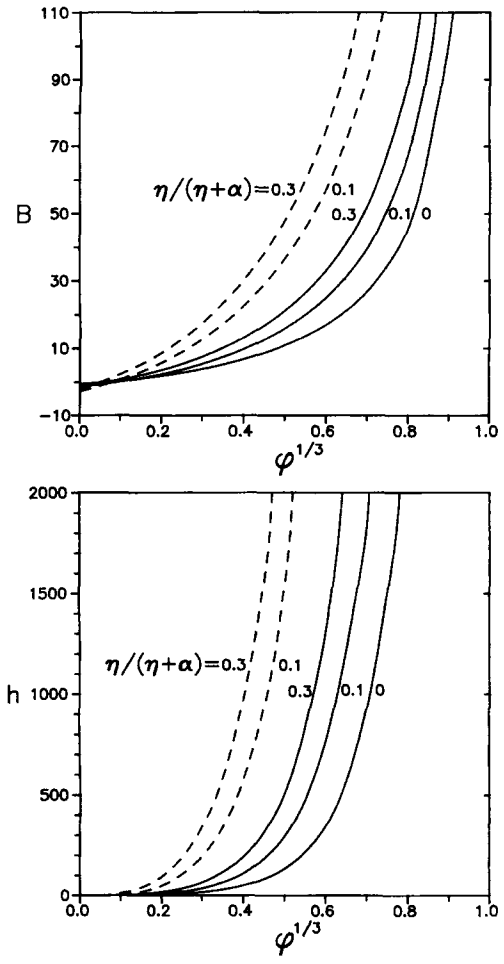

Fig. 1 The parameters B and h for the motion of a swarm of polymer-coated spheres relative to a fluid as a function of $\varphi^{1/3}$ with $\beta_0 = 100$ in the free-draining limit ($f = 1$). The solid curves are plotted for the case of $\alpha = 0.5$ and the dashed curves are plotted for the case of $\alpha = 0.25$

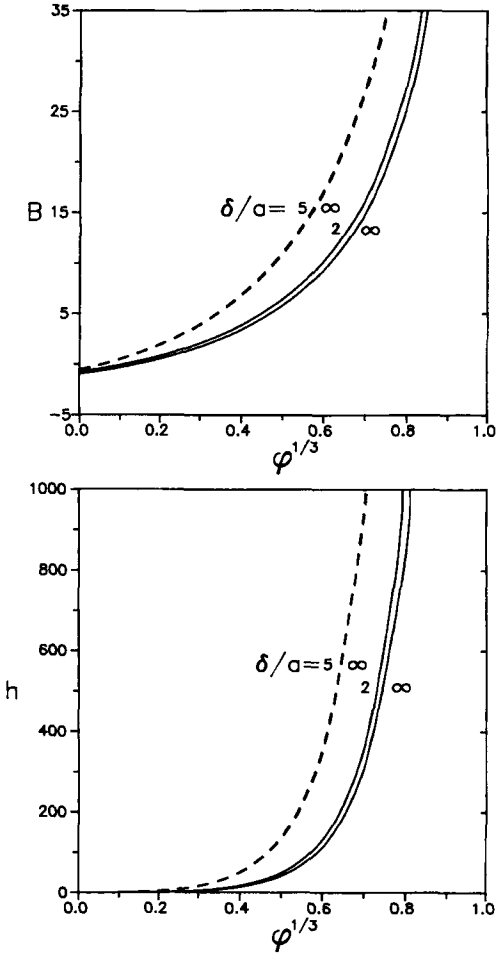

Fig. 2 The parameters B and h for the motion of a swarm of polymer-coated spheres relative to a fluid as a function of $\varphi^{1/3}$. The solid curves are plotted for the case of $\beta_0 = 10$ and the dashed curves are plotted for the case of $\beta_0 = 100$. Note that $\delta/a \to \infty$ represents the free-draining limit ($f = 1$) and the two dashed curves are almost indistinguishable

Kim [17] and use a combination of a modified Brinkman equation at low ϕ and the Blake–Kozeny equation at high ϕ for the expression of function $f(\phi)$:

$$f = \begin{cases} 1 + 2.121\phi^{1/2} + 0.84\phi \ln \phi + 16.45\phi & \text{for } \phi < 0.29 \,, \\ \dfrac{8.34\phi}{(1-\phi)^3} & \text{for } \phi > 0.29 \,, \end{cases} \tag{43a,b}$$

where $\phi = (4/3)\pi a^3 \rho(y)$. The ratio A/A_∞ (or g/A_∞) is independent of $f(\phi)$ (in spite of the fact that A_∞ is a weak function of δ/a) and its results are the same as those given in Table 1. In Fig. 2, the results of parameters B and h versus $\varphi^{1/3}$ obtained using Eq. (43) are plotted for several values of β_0 and δ/a. Although the particle interaction effect on B and h is increased when the value of δ/a is decreased for a given value of β_0, the hydrodynamic interactions among the polymer segments produce relatively small effects on B and h.

Concluding remarks

The slow motion of a swarm of identical spherical particles coated with adsorbed polymer layers relative to a fluid has been analyzed using a cell model in this work. The analysis provides simple equations which must be solved, given the polymer segment density distribution $\rho(y)$ and rheological parameters $\mu(y)$ and $\beta(y)$, to determine the parameters A and B of Eq. (9) or parameters g and h of Eq. (30) as

required by Eq. (33). The hydrodynamic force exerted on a particle can be calculated using Eq. (8) and the results of A and B, which is correct to $O(\lambda^2)$. For the exponential polymer segment distribution given by Eq. (40), the ratio A/A_∞ or g/A_∞ is found to be independent of the values of β_0, δ/a, α, and $\eta/(\eta+\alpha)$, and its results for various values of φ are listed in Table 1. The dependence of B and h on β_0, δ/a, α, $\eta/(\eta+\alpha)$, and $\varphi^{1/3}$ is given in Table 1 and Figs. 1 and 2. The results indicate that the particle interaction effects on the motion of an assemblage of polymer-coated particles relative to a fluid can be significant.

Throughout the calculations in the previous section we have assumed a simple exponential decay of the polymer segment density. This could be an oversimplification since the convex nature of the surfaces of the particles might adjust the excluded volume effects among the polymer segments. A segment density of the following form was suggested [17] to allow for curvature effects on polymer distribution:

$$\rho(y) = \rho_0 \frac{e^{-y/\delta}}{1 + s(y/R_1)}, \tag{44}$$

where s should be a positive value. For systems with no tails in the free-draining limit, $\beta(y)$ has the form of the above equation with ρ_0 replaced by β_0. It is understood that parameters A_∞ and A (or g) are independent of the curvature coefficient s. We have numerically solved Eqs. (26) and (27) with the segment distribution given by Eq. (44), and substituted the solution of G and H into Eq. (28b) to compute parameters B and h. These calculations, which are plotted in Fig. 3, indicate that the values of B and h decrease with the increase of s for various values of φ as one would expect.

One may wish to consider a polymer segment distribution that has the same adsorbed amount as for the exponential distribution but is uniform over a distance from the particle surface:

$$\rho(y) = \begin{cases} \rho_0 & \text{if } 0 \le y \le \delta, \quad (45a) \\ 0 & \text{if } y > \delta. \quad (45b) \end{cases}$$

For this profile in the free-draining limit, $\beta(y)$ has the form of Eq. (45) with ρ_0 replaced by β_0 and it can be shown that

$$A_\infty = 1 - \beta_0^{-1/2} \tanh \beta_0^{1/2},$$

$$B_\infty = -\frac{1}{A_\infty \beta_0}(1 - \operatorname{sech} \beta_0^{1/2})^2. \tag{46a,b}$$

It can be found that the value of A_∞ is about six times greater (if $\beta_0 \approx 100$) for an exponential distribution of segments than for the polymer uniformly distributed over a region of thickness δ. Although A_∞ is a function of β_0 for this segment distribution, the ratio A/A_∞ or g/A_∞ is independent of the segment distribution and its results have been given in Table 1. In Fig. 4, the numerical results of parameters B and h for the motion of a swarm of polymer-coated spheres relative to a fluid versus $\varphi^{1/3}$ obtained using Eq. (45) for the segment distribution are plotted. The corresponding results for the case of an exponential distribution of segments are also plotted in the same figure for comparison. It can be seen that the particle interaction effect on B and h is much weaker for the uniform distribution of segments over a distance from the particle surface than for the exponential distribution of segments.

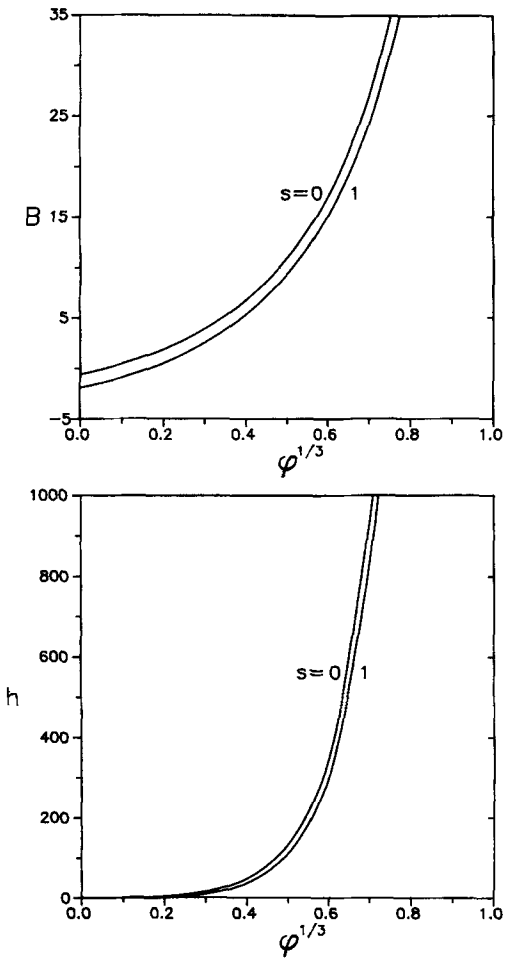

Fig. 3 The parameters B and h for the motion of a swarm of polymer-coated spheres relative to a fluid as a function of $\varphi^{1/3}$ with the segment density distribution given by Eq. (44) and $\beta_0 = 100$ in the free-draining limit

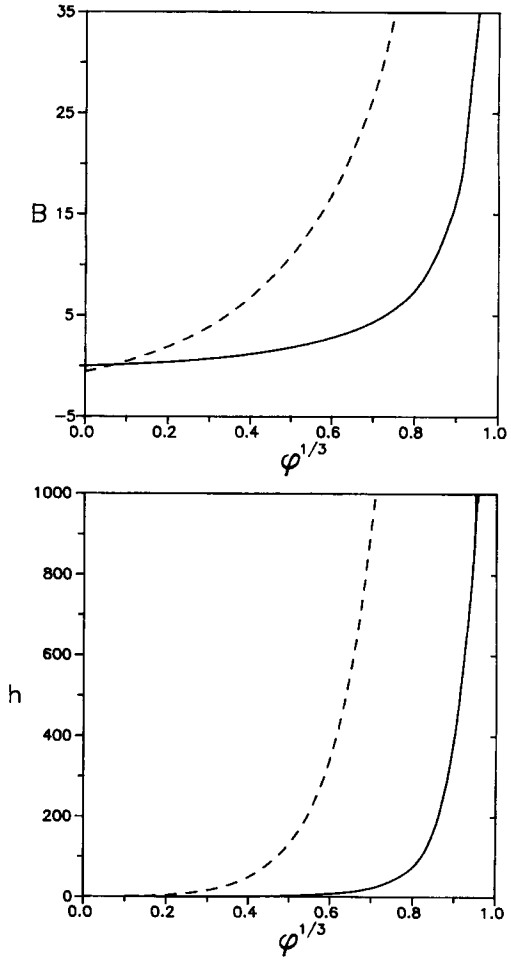

Fig. 4 The parameters B and h for the motion of a swarm of polymer-coated spheres relative to a fluid as a function of $\varphi^{1/3}$ with the segment density distribution given by Eq. (45) and $\beta_0 = 100$ in the free-draining limit. The corresponding results for the exponential segment distribution are also plotted by dashed curves for comparison

Acknowledgements This work was supported by the National Science Council of the Republic of China.

Appendix: An approximate solution for the mean settling velocity in a suspension of polymer-coated spheres

Based on a microscopic model of two-particle interactions in a dilute dispersion which involves both statistical and low Reynolds number hydrodynamic concepts [19, 20], the mean settling velocity in a bounded suspension of identical polymer-coated spheres (having radius R_1 and volume fraction φ) can be expressed as

$$U = U_\infty[1 + v\varphi + O(\varphi^2)] , \tag{A1}$$

with

$$v = -(2 + 3\kappa) + 8\int_0^1 \{[M_{11}^{(p)} + 2M_{11}^{(n)} - 3] + [M_{12}^{(p)} + 2M_{12}^{(n)} - \tfrac{3}{2}\kappa w]\} w^{-4}\,dw . \tag{A2}$$

Here,

$$\kappa = 1 + A_\infty\lambda + A_\infty B_\infty\lambda^2 + O(\lambda^3) , \tag{A3}$$

w is the ratio of the particle diameter to the center-to-center distance between two particles, and $M_{11}^{(p)}$, $M_{12}^{(p)}$, $M_{11}^{(n)}$, and $M_{12}^{(n)}$ are the mobility coefficients accounting for the hydrodynamic interactions between two particles.

Using a far-field approximate technique, Anderson and Solomentsev [18] derived the following formulas for the mobility coefficients:

$$M_{11}^{(p)} = 1 - \tfrac{15}{64}[1 + 4A_\infty\lambda + (6A_\infty^2 + 7A_\infty B_\infty)\lambda^2]w^4 + O(\lambda^3, w^6) , \tag{A4a}$$

$$M_{12}^{(p)} = \tfrac{3}{4}(1 + A_\infty\lambda + A_\infty B_\infty\lambda^2)w - \tfrac{1}{8}[1 + 3A_\infty\lambda + \tfrac{3}{2}(A_\infty^2 + A_\infty B_\infty - 2\Omega_\infty)\lambda^2]w^3 + O(\lambda^3, w^7) , \tag{A4b}$$

$$M_{11}^{(n)} = 1 + O(\lambda^3, w^6) , \tag{A4c}$$

$$M_{12}^{(n)} = \tfrac{3}{8}(1 + A_\infty\lambda + A_\infty B_\infty\lambda^2)w + \tfrac{1}{16}[1 + 3A_\infty\lambda + \tfrac{3}{2}(A_\infty^2 + A_\infty B_\infty - 2\Omega_\infty)\lambda^2]w^3 + O(\lambda^3, w^7) , \tag{A4d}$$

where

$$\Omega_\infty = \frac{1}{R_1}\int_0^\infty (G_\infty + y - R_1\gamma_\infty)\,dy . \tag{A5}$$

In Eq. (A.5), G_∞ and γ_∞ are the values of G and γ defined by Eqs. (25a) and (22) as $R_2/R_1 \to \infty$. When the segment density distribution in the adsorbed polymer layer is given by Eq. (40) or Eq. (45), it can be shown that $\Omega_\infty = -(A_\infty^2 - A_\infty B_\infty)/2$.

Substituting Eq. (A.4) into Eq. (A.2) and performing the integration leads to

$$v = -\tfrac{55}{8} - \tfrac{9}{2}A_\infty\lambda - \tfrac{9}{8}(10A_\infty^2 + 9A_\infty B_\infty)\lambda^2 + O(\lambda^3) . \tag{A6}$$

This expression is not exact because $O(w^6)$ terms in Eq. (A4) are neglected in the calculations. For a suspension of identical "bare" spheres ($\lambda = 0$), Eq. (A6) gives $v = -55/8$, in agreement with the analytical result of the

same accuracy obtained by Keh and Chen [27]. Similar to Eq. (33), Eqs. (A1) and (A6) can also be applied to the case of fluid flow through a bed of polymer-coated spheres. Both Eqs. (33) and (A6) predict that the value of U/U_∞ decreases monotonically from unity with the increase of φ from zero. Note that U/U_∞ varies linearly with φ in Eq. (A1), while U/U_∞ depends linearly with $\varphi^{1/3}$ in Eq. (33) according to the relations given by Eq. (39).

References

1. Hoeve CAJ (1966) J Chem Phys 44:1505–1509
2. Roe RJ (1966) J Chem Phys 44:4264–4272
3. Hesselink FTh (1975) J Colloid Interface Sci 50:606–608
4. Scheutjens JMHM, Fleer GJ (1980) J Phys Chem 84:178–190
5. deGennes PG (1980) Macromolecules 13:1069–1075
6. Anderson JL, McKenzie PF, Webber RM (1991) Langmuir 7:162–166
7. Stromberg RR, Tutas DJ, Passaglia E (1965) J Phys Chem 69:3955–3963
8. Doroszkowski A, Lambourne R (1968) J Colloid Interface Sci 26:214–221
9. Garvey MJ, Tadros ThF, Vincent B (1976) J Colloid Interface Sci 55:440–453
10. Kozicki W, Hanna MR, Tiu C (1988) J Rheology 32:593–619
11. Baker JA, Pearson RA, Berg JC (1989) Langmuir 5:339–342
12. Carvalho BL, Tong P, Huang JS, Witten TA, Fetters LJ (1993) Macromolecules 26:4632–4639
13. Napper DH (1983) Polymeric Stabilization of Colloidal Dispersions. Academic Press, London
14. McKenzie PF, Kapur V, Anderson JL (1994) Colloids Surfaces A 86:263–272
15. Kawaguchi M, Takahashi A (1992) Adv Colloid Interface Sci 37:219–317
16. Varoqui R, Dejardin P (1977) J Chem Phys 66:4395–4399
17. Anderson JL, Kim J (1987) J Chem Phys 86:5163–5172
18. Anderson JL, Solomentsev Y (1996) Chem Eng Comm 148–150:291–314
19. Batchelor GK (1972) J Fluid Mech 52:245–267
20. Reed CC, Anderson JL (1980) AIChE J 26:816–827
21. Happel J (1958) AIChE J 4:197–201
22. Kuwabara S (1959) J Phys Soc Jap 14:527–533
23. Happel J, Brenner H (1983) Low Reynolds Number Hydrodynamics. Martinus Nijhoff, The Netherlands
24. Dassios G, Handjinicolaou M, Coutelieris FA, Payatakes AC (1995) Int J Eng Sci 33:1465–1490
25. Fleer GJ, Cohen Stuart MA, Scheutjens JMHM, Cosgrove T, Vincent B (1993) Polymers at Interfaces. Chapman & Hall, London
26. Gerald CF, Wheatley PO (1994) Applied Numerical Analysis, 5th ed. Addison-Wesley, Reading, MA
27. Keh HJ, Chen SH, Chem Eng Sci (in press)